

191  
3-24-92 JS (2)

LBL-30707  
UC-814



# Lawrence Berkeley Laboratory

UNIVERSITY OF CALIFORNIA

## EARTH SCIENCES DIVISION

### Waste-Package Release Rates for Site Suitability Studies

W.W.-L. Lee, M.M. Sadeghi, P.L. Chambré, and T.H. Pigford

April 1991



#### DISCLAIMER

This document was prepared as an account of work sponsored by the United States Government. Neither the United States Government nor any agency thereof, nor The Regents of the University of California, nor any of their employees, makes any warranty, express or implied, or assumes any legal liability or responsibility for the accuracy, completeness, or usefulness of any information, apparatus, product, or process disclosed, or represents that its use would not infringe privately owned rights. Reference herein to any specific commercial product, process, or service by its trade name, trademark, manufacturer, or otherwise, does not necessarily constitute or imply its endorsement, recommendation, or favoring by the United States Government or any agency thereof, or The Regents of the University of California. The views and opinions of authors expressed herein do not necessarily state or reflect those of the United States Government or any agency thereof or The Regents of the University of California and shall not be used for advertising or product endorsement purposes.

This report has been reproduced directly  
from the best available copy.

Available to DOE and DOE Contractors  
from the Office of Scientific and Technical Information  
P.O. Box 62, Oak Ridge, TN 37831  
Prices available from (615) 576-8401, FTS 626-8401

Available to the public from the  
National Technical Information Service  
U.S. Department of Commerce  
5285 Port Royal Road, Springfield, VA 22161

Lawrence Berkeley Laboratory is an equal opportunity employer.

LBL--30707

DE92 009131

## Waste-Package Release Rates for Site Suitability Studies

*W. W.-L. Lee, M. M. Sadeghi, P. L. Chambré, and T. H. Pigford*

Department of Nuclear Engineering  
University of California

and

Earth Sciences Division  
Lawrence Berkeley Laboratory  
University of California  
Berkeley, California 94720

April 1991

This work was supported by the Director, Office of Civilian Radioactive Waste Management, Yucca Mountain Site Characterization Project, of the U.S. Department of Energy under Contract No. DE-AC03-76SF00098.

**MASTER**

*EP*

**The authors invite comments and would appreciate  
being notified of any errors in the report.**

**T. H. Pigford  
Department of Nuclear Engineering  
University of California  
Berkeley, CA 94720**

## CONTENTS

INTRODUCTION . . . . .	1
DATA AND PARAMETERS . . . . .	1
RESULTS . . . . .	3
1. Wet-Drip Water-Contact Mode, Bathtub Model . . . . .	3
1.1 The Wet-Drip Bathtub Model . . . . .	3
1.2. Wet-Drip Release of Soluble Species . . . . .	4
1.3. Wet-Drip Release of Low-Solubility Species . . . . .	4
2. The Wet-Continuous Water Contact Mode . . . . .	5
2.1 The Wet-Continuous Model . . . . .	5
2.2 Diffusive Release of Soluble Species . . . . .	6
2.3 Diffusive Release of Low-Solubility Species . . . . .	6
2.4 Effect of Water Flow in Fractures . . . . .	7
3. Release From a Borehole Intersecting a Waste Package . . . . .	8
References . . . . .	8

## INTRODUCTION

Performance-assessment calculations in support of the site-suitability effort for the Yucca Mountain Project will address radionuclide transport arising from various disruptive scenarios. Here we present release rates of radionuclides from individual waste packages for scenarios involving various postulated forms of water intrusion, including increased infiltration rate as well as rock immediately surrounding an individual waste package becoming saturated with ground water. We examine:

1. Effect of increased water infiltration rate on release rates.
2. Increases in radionuclide release rates resulting from water filling the annulus between the waste container and the surrounding rock, as well as water saturating the pores and fractures in the rock surrounding the waste package.
3. The effect of flow in fractures in the saturated rock on release rate.
4. Release of radionuclides to the mountain surface resulting from an exploratory borehole shaft intersecting a waste package.

The radionuclides considered are Tc-99; I-129; Cs-135; Np-237; Pu-239,240,242; and Am-241,243.

Release rates are calculated for both the wet-drip bathtub and the wet-continuous water-contact modes, as described in the Working Group 2 report [Apted *et al.* 1990], applying equations as published by Sadeghi, *et al.*, [1990] and as extended in the present report.

## DATA AND PARAMETERS

Parameters used in these plots are the same as in the 1990 Working Group 2 Report [Apted *et al.* 1990] except for the retardation coefficients. The waste package parameters selected for the present analysis are given in Table I.

**Table I. The Reference Waste Package**

Waste Package Height	4.6 m
Waste Package Outside Diameter	0.71 m
Waste Package Overall Volume	1.73 m <sup>3</sup>
Waste Package Internal Void Volume	1.22 m <sup>3</sup>
Waste Package Content	2.1 Mg U fuel (2.1 MTHM)
Surface area of waste container	11 m <sup>2</sup>
Air gap between container and tuff	3 cm

Hydrological properties used in these calculations are given in Table II.

**Table II. Hydrological Properties**

Far-field average Darcy velocity of ground water	0.5, 0.1 and 0.05 mm/a
Porosity of intact tuff and of pieces of tuff rubble	0.16
Water saturation of intact tuff and of pieces of tuff rubble (when unsaturated)	0.86
Diffusion coefficient in water continuum	$3.15 \times 10^{-2} \text{ m}^2/\text{a}$
Void fraction in annulus (volume of air/total volume of annulus)	0.30

Table III shows the characteristics of the nuclides studied. Elemental solubilities have been estimated from concentrations of the actinides in the spent-fuel leaching experiments of Wilson [1990].

**Table III. Radionuclide Characteristics**

Nuclide	Half Life (a)	1000-a inventory (Ci)	Elemental Solubility (g/m <sup>3</sup> )
Tc-99	$2.11 \times 10^5$	$2.73 \times 10^1$	Not used
I-129	$1.57 \times 10^7$	$6.61 \times 10^{-2}$	Not used
Cs-135	$2.30 \times 10^6$	$7.24 \times 10^{-1}$	Not used
Np-237	$2.14 \times 10^6$	2.19	$3.0 \times 10^{-4}$
Pu-239	$2.41 \times 10^4$	$6.41 \times 10^2$	$9.5 \times 10^{-4}$
Pu-240	$6.56 \times 10^3$	$1.00 \times 10^3$	$9.5 \times 10^{-4}$
Pu-242	$3.73 \times 10^5$	3.61	$9.5 \times 10^{-4}$
Am-241	$4.33 \times 10^2$	$1.88 \times 10^3$	$3.8 \times 10^{-5}$
Am-243	$7.38 \times 10^3$	$3.28 \times 10^1$	$3.8 \times 10^{-5}$

Retardation coefficients are obtained from experimental sorption ratios (Table IV) in the *Site Characterization Plan* [USDOE 1988]. The sorption coefficients are averaged values from six tuff samples in the Topopah Spring member of the Paintbrush tuff, the potential repository horizon. To calculate the sorption retardation coefficient for transport in unsaturated porous rock, assuming local chemical equilibrium between a species in the pore liquid and that same species sorbed in the rock, the retardation coefficient  $K$  is given by

$$K = 1 + \frac{1 - \epsilon_r}{\epsilon_r \Psi} \rho K_d \quad (1)$$

where  $K_d$  is the dimensionless distribution coefficient (mass per unit volume of rock solid divided by mass per unit volume of pore liquid)

$\rho$  is the bulk density

$\epsilon_r$  is the overall porosity of the rock matrix

$\Psi$  is the fractional saturation of the rock matrix. To calculate the unsaturated retardation coefficient, a porosity of 0.16, an ambient saturation of 0.86 and a bulk density of 2.5 g/cm<sup>3</sup> have been used. Table V identifies the boreholes and the depth from which these samples are taken. The locations of the boreholes are shown in the *Site Characterization Plan* [USDOE 1988].

**Table IV. Data for Sorption Ratios**

	Sorption ratio (ml/g)	Retardation coefficient
Technetium	0.16	3.4
Iodine	0	1
Cesium	417	6360
Uranium	1.8	28
Neptunium	4.9	76
Plutonium	208	3180
Americium	1070	16300

**Table V. Data Source for Sorption Ratios**

Tuff Sample Number	From Borehole	Depth (m)
G1-1292	USW G-1	393.7
GU3-1203	USW GU-3	366.6
GU3-1301	USW GU-3	396.4
JA-18	J-13	432.7
YM-22	UE25a#1	258.4
YM-30	UE25a#1	385.1

## RESULTS

### 1. Wet-Drip Water-Contact Mode, Bathtub Model

#### 1.1 The Wet-Drip Bathtub Model

The wet-drip water-contact mode assumes that water drips through cracks at the top of a failed waste container. In the bathtub model the water slowly fills the container and reacts with the spent fuel. The Zircaloy cladding is conservatively assumed not to interfere with fuel-water reaction. Water containing



dissolved radionuclides rises slowly within the container and is at all times well mixed by convection. After reaching the top, where the container penetrations are assumed to occur, the contaminated water overflows and is assumed to drip directly onto the rock below the container. The outflowing drip is expected to move quickly through voids in any rubble that may be present in the annulus between the container and the borehole.

For water dripping into boreholes, we use the water flux passing through a cross-sectional area above the borehole. Disturbances from the repository or variations in local hydrologic properties would in some cases divert water away from the borehole, but perhaps in some cases divert water toward the borehole. We assume a larger "catchment area" of radius two times the borehole radius. Thus the volume rate of flow of ground water that drips onto and into a container is assumed to be the product of the Darcy infiltration rate and four times the cross-sectional area of the borehole.

### **1.2. Wet-Drip Release of Soluble Species**

The time-dependent rates of release of the soluble species Tc-99, I-129, and Cs-135 depend on the alteration rate of the spent fuel in contact with water and the time for water to fill the container. Darcy infiltration rates of 0.05, 0.1, and 0.5 mm/a are assumed. Results, shown in Figure 1, are presented as the fractional release rate as function of time since first intrusion of water into the waste container. The fractional release rate is the mass rate of release of a species divided by the inventory of that species at 1,000 years. During the times shown here decay is small, so the curves for the three soluble species are essentially identical. Each curve, for a given infiltration rate, begins at the time of first overflow.

Figure 1 shows the wet-drip fractional release rates of soluble species, due to alteration of the waste matrix. The peak release rates occur soon after the container begins to overflow. The peak release rates are near the experimental fractional alteration rate of the waste matrix [Wilson 1990]. The time for first release is inversely proportional to the infiltration rate. A small fraction of these soluble species will be present in the fuel-cladding gap, fuel gas plenum, and accessible grain boundaries. This "gap activity" can dissolve in container water more rapidly than the soluble species still present in the fuel matrix. However, for the wet-drip bathtub scenario this "gap activity" contributes much less to release rate to the rock than does the dissolution of soluble species from alteration of the spent fuel matrix [Apted *et al.* 1990].

These results are for a single waste package. If container failures are distributed with respect to location and time, those distributions must be included in evaluating the net source term for the repository.

### **1.3. Wet-Drip Release of Low-Solubility Species**

The rates of release of isotopes of neptunium, plutonium, and americium are found to be limited by elemental solubilities. Results are shown in Figures 2, 3, and 4, which are plots of fractional release rates as a function of time since first water intrusion into the waste container. For an element with a single predominant isotope,

such as Np-237, the release rate is constant over time after the first overflow from the failed container and is proportional to the infiltration rate, as shown in Figure 2.

As shown in Figure 3, the fractional release rate of Pu-240 decreases with time because of radioactive decay. As it decays its concentration is a smaller fraction of the plutonium solubility. Because of the early decay of Pu-240, the isotopic fraction and concentration of Pu-239 first increase with time and then decrease because of Pu-239 decay. As Pu-239,240 decay, Pu-242 becomes the predominant isotope. Its release rate increases with time because its concentration increases and finally equals the elemental solubility. As in the case of Np-237, the effect of different water infiltration rates is to change the time of appearance of the first release into the surrounding rock.

As shown in Figure 4, the fractional release rate of Am-241 decreases rapidly with time because of its short half life, soon resulting in a constant release rate of Am-243.

For these wet-drip calculations the isotopic fractions of plutonium and of americium at the time of water intrusion were assumed to equal the isotope fractions at 1000 years. The actual isotopic fractions to use depend on the time for first water intrusion into a failed container. For chronological times in the range of 0 to 10,000 years, the isotopic fractions of Pu-240 and Am-241 can change considerably, depending on the time for first water intrusion. Corrections are not made for the purpose of this document because these two isotopes are usually not the principal ones in determining hazards from hydrogeologic transport.

## **2. The Wet-Continuous Water Contact Mode**

### **2.1 The Wet-Continuous Model**

The wet-continuous model considers diffusive/convective transport of dissolved radionuclides from spent fuel that is in contact with ground water. Here the container is assumed to have extensively failed, so that it presents no barrier to the diffusion of dissolved species from the waste surface into the surrounding rock. In the Working Group 2 report [Apted *et al.* 1990] we were estimating the release rate for a waste package surrounded by unsaturated rock. It was conservatively assumed that those pores in the rock matrix that contained ground water were interconnected and provided continuous diffusion pathways for the transport of dissolved radionuclides. Also, the thin annulus between the waste container and the borehole was assumed to be filled with rubble, which provided diffusive pathways through pores in the individual rubble pieces. Because of the limited areal contact between individual rubble pieces, an effective diffusion coefficient for the rubble was expected to be several orders of magnitude below that of intact rock. Thus, the rubble zone was expected to provide a formidable barrier to diffusive transport from the waste to the intact rock, as long as the rock is unsaturated. As for the wet-drip case, the release rate is calculated at the borehole wall.

In the intrusion scenarios considered here the rock surrounding an individual waste package is assumed to be saturated, so that the annulus can contain water or a rubble-water mixture. In either case, the extensive

water phase in the annulus will effectively short circuit the tortuous diffusion pathways of the rubble and will thereby increase the diffusive release rate. This is the major effect of local saturation on the release rate.

Here we first present diffusive wet-continuous release rates for saturated rock, for  $\Psi = 1$  in (1), still neglecting the effect of water flow on mass transfer. The effect of water flow in fractures, that could also accompany saturation, will be considered in a later section.

## **2.2 Diffusive Release of Soluble Species**

The diffusive wet-continuous release rates for the soluble species, Tc-99, I-129, and Cs-135, that are released congruently with fuel-matrix alteration, are shown in Figure 5. Also shown, for comparison, are the moist-continuous release rates for unsaturated rock and rubble. In both sets of curves the different radionuclides fall on different curves because of differences in retardation. The effect of water intrusion is to short-circuit the rubble zone and increase the peak release rates of Tc-99 and I-129 by about an order of magnitude and to increase the peak release rate of Cs-135 by about one hundred-fold. Also, because diffusional resistance in the rubble no longer delays transport to the intact rock, the radionuclides appear much sooner in the intact rock. Without retardation by the rubble zone, the Cs-135 peak appears along with the peaks of Tc-99 and I-129 at the end of the alteration period. The peak fractional release rates are close to the fractional alteration rate of the fuel matrix. Here the Cs-135 does not experience the diffusive dispersion that occurs when transport must occur by diffusion through the rubble.

These release-rate curves and tabulated data show the release rates for a single waste package, as a function of time after water contact begins.

## **2.3 Diffusive Release of Low-Solubility Species**

The diffusive fractional release rates of isotopes of the low-solubility actinides are shown in Figure 6 for Np-237, in Figure 7 for Pu-239,240,242, and in Figure 8 for Am-241,243. Also shown are the diffusive release rates for the moist-continuous condition, with a large diffusive impedance in the rubble zone. Here saturation by water intrusion increases the release rates by about two orders of magnitude, and first releases into the rock occur soon after water contact has begun.

The fractional release rates of Am-241,243 are greater than for the other actinides because of the low mass inventory of americium in the waste.

We have shown elsewhere [Pigford and Chambré 1988] that for the infiltration rates assumed in this study, the diffusive release rates are little affected by infiltration rate.

Comparing the results for Np-237 in Figure 6 with those in Figure 2, we see that the diffusive release is several orders of magnitude larger than the bulk-flow solubility-limited release rate of the wet-drip model, even at the highest infiltration rates considered here. This is also true for the isotopes of plutonium and americium.

Therefore, for the most conservative calculations, the release rates from the wet-continuous water-contact mode should be used.

## 2.4 Effect of Water Flow in Fractures

The diffusive releases calculated in Sections 2.2 and 2.3 are calculated on the basis of diffusion into water-filled pores in the surrounding rock. Any porosity associated with fractures that intersect the borehole is included in this calculation. The diffusive pathways are predominantly into the rock matrix, because of the high (0.16) porosity of the matrix and because there is far more volume of rock matrix than of fractures. However, it is reasonable to expect that ground water flowing in the fractures can increase the transport of radionuclides from the waste.

We consider a planar fracture with parallel walls that intersects a borehole containing a waste package, illustrated schematically in Figure 9. We assume one fracture intersecting a waste package emplacement borehole, and we assume that the fracture plane is normal to the axis of the cylindrical waste. We calculate the rate of diffusive-advective transport of a solubility-limited species directly into the fracture, where the fracture intersects the borehole, by applying the steady-state form of the mass-transfer rate from the surface of a cylinder to water flowing in potential flow around the cylinder, as derived by Chambré [1982]. Here we assume that fracture water is similarly diverted as it intersects and flows around the filled borehole. Effect of flow in the rubble-filled or open annulus between the waste container and the borehole walls will be considered in a later supplement. The analytic solution for the mass transfer rate for a long-lived species is

$$\dot{m} = \frac{16}{\sqrt{\pi}} b D c_s \epsilon \sqrt{Pe} \quad (2)$$

where

$\dot{m}$  is the mass transfer rate (g/a)

$2b$  is the fracture aperture

$V$  is the upstream pore velocity of ground water in the fracture

$R$  is the borehole radius

$D$  is the diffusion coefficient for water in the fracture

$\epsilon$  is the porosity of sediments within the fracture

$c_s$  is the solubility of the species

The equation is applicable to sufficient accuracy for the Peclet number  $Pe$  equal to or greater than four, where

$$Pe = \frac{VR}{D} \quad (3)$$

In Figure 10 we show the mass release rate of Np-237 directly into the fractures as a function of the Peclet number, for various values of the fracture aperture. Also shown is the diffusive release rate into the rock

matrix, which is affected little by water flow rate in the fracture. Here we adopt the average diffusive release rate from Figure 6, evaluated for the interval 1,000 to 10,000 years. Clearly, because of the large porosity of the rock matrix, the diffusive release rate is far greater than the rate of advective release into the fracture, for Pe even as high as 1,000, corresponding to very fast flow in a fracture. For example, for a borehole radius of 0.385 m, as used in these calculations, Peclet of 1,000 corresponds to a fracture pore velocity of 82 m/a.

In Figure 11 we show the estimated total release rate of Np-237 in the 1,000–10,000-a interval, as a function of Peclet number. The corrections for fracture flow are so small that for the purposes of the site suitability studies it should be sufficient to use the results of the diffusive release calculations shown in Section 2.3. The diffusive release becomes even more important during the earlier transient period. If water flow in the locally saturated repository occurs mainly within fractures, the diffusive release to the rock matrix eventually appears in the fracture water as a source for far-field transport.

Similar calculations of the effect of fracture flow on release rates of the plutonium and americium isotopes show that the release rate to fractures, with fracture-flow, is small compared to the release rate to the rock matrix by diffusion. Therefore we recommend that the results of the diffusive-release calculations of Section 2.3 be used for the site-suitability studies.

For similar reasons, fracture flow cannot significantly affect the release rates of the soluble species. The peak release rates of these species are governed by the chemical alteration rate of the spent-fuel matrix and, within the framework of the phenomena modeled herein, cannot be affected by fracture flow. Fracture flow could affect the release rates far from the peaks, but the effects cannot be large, for the same reasons as given above for the effect of fracture flow on the release rates of the low-solubility species. Therefore, we recommend that the diffusive release rates calculated in Section 2.2 be used for the site-suitability studies.

In the foregoing analysis, we have assumed only one fracture intersecting a waste package. At Yucca Mountain the potential repository horizon is the Topopah Springs welded tuff, a highly fractured unit. Any one waste-emplacment borehole may be intersected by more than one fracture. Table VI shows the fracture porosity of two samples from the Topopah Springs welded unit, one upper and one lower.

**Table VI. Fracture Porosity of Topopah Spring Welded Unit**

Core Sample	Fracture Porosity
Tsw (upper)	$4.1 \times 10^{-5}$
Tsw (lower)	$1.8 \times 10^{-4}$

Source: Birdsell and Travis [1991]

Fracture porosity is the product of fracture volume and the number of fractures per unit volume of rock.

Assuming planar fractures each spanning an average surface of  $1 \text{ m}^2$  per  $\text{m}^3$  of rock, we use the fracture porosity of Table VI to calculate the fracture density for a given fracture aperture, and the result is Table VII.

**Table VII. Fracture Density Calculated from Fracture Aperture**

Postulated Fracture Aperture	Fractures/ $\text{m}^3$	
	T <sub>Sw</sub> (upper)	T <sub>Sw</sub> (lower)
$1 \times 10^{-5} \text{ m}$	4.1	18
$1 \times 10^{-4} \text{ m}$	0.41	1.8
$1 \times 10^{-3} \text{ m}$	0.041	0.18

Another source, Montazer and Wilson [1984], gives the fracture density as 8 to 40 per  $\text{m}^3$ .

The current design waste emplacement borehole is 0.385 m in radius and 4.6 m high, with a volume of 0.536  $\text{m}^3$ . Thus the number of fractures intersecting a borehole might range from 20 of  $1 \times 10^{-5} \text{ m}$  aperture to 0.02 of the  $1 \times 10^{-3} \text{ m}$  aperture. Thus, for 20 fractures, each of  $10^{-5} \text{ m}$  aperture, and using the single-fracture results from Figure 10, the total mass-transfer rate into fractures will still be two orders of magnitude below the diffusive release into the tuff matrix, for  $Pe \leq 70$ . For fractures of  $10^{-4} \text{ m}$  aperture, the ten-fold fewer intersecting fractures, for the same fracture porosity, results in the same result as for the  $10^{-5} \text{ m}$  fractures. For  $10^{-3} \text{ m}$ -aperture fractures, less than one fracture is expected to intersect an emplacement hole.

From this analysis, we conclude that for the range of parameters considered here mass transfer into fractures is less than mass transfer directly into tuff surrounding a waste emplacement borehole.

### **3. Release From a Borehole Intersecting a Waste Package**

Postulated future inadvertent intrusion into the repository by exploratory drilling might intersect a waste package and bring the contents to the surface. Conservatively assuming that the drill macerates the entire content of a waste package, the amount and composition of the radioactive material brought to the surface is given by the contents of a single waste package. The inventories of individual radionuclides from a single waste package, as a function of time since waste emplacement, are given in Table VIII.

#### **Note**

All calculated results can also be obtained from the authors in tabular form on electronic media.

#### **References**

M. J. Apted, W. J. O'Connell, K. H. Lee, A. T. MacIntyre, T.-S. Ueng, T. H. Pigford and W. W.-L. Lee,

1990. "Preliminary Calculations of Release Rates of Tc-99, I-129, Cs-135, & Np-237 from Spent Fuel in a Tuff Repository," WG2-5-90, PNL/LLNL/LBL Report.

K. H. Birdsall and B. J. Travis, 1991. *Results of the COVE2a Benchmarking Calculations Run with TRACR3D*, Report LA-11513-MS.

P. L. Chambré, T. H. Pigford, A. Fujita, T. Kanki, A. Kobayashi, H. Lung, D. Ting, Y. Sato, and S. J. Zavoshy, 1982. *Analytical Performance Models*, Report LBL-14842.

P. Montazer and W. E. Wilson, 1984. *Conceptual Hydrologic Model of Flow in the Unsaturated Zone*, Report USGS-WRI-84-4345.

T. H. Pigford and P. L. Chambré, 1988. "Near-Field Mass Transfer in Geologic Disposal Systems: A Review." in *Scientific Basis for Nuclear Waste Management XI*, eds. M.J. Apted and R.E. Westerman, Materials Research Society, Pittsburgh, PA, 125.

M. M. Sadeghi, T. H. Pigford, P. L. Chambré and W. W.-L. Lee, 1990. "Equations for Predicting Release Rates for Waste Packages in Unsaturated Tuff," Report LBL-29254.

U.S. Department of Energy, 1988. "Site Characterization Plan, Yucca Mountain Site, Nevada Research and Development Area, Nevada," DOE/RW-0199.

C. N. Wilson, 1990. "Results from NNWSI Series 3 Spent Fuel Dissolution Tests," Report PNL-7170.

Table VIII. Inventory of a waste container exhumed at these times

Nuclide	Half Life (a)	I at 10 a (Ci/Mg U)	10 (Ci)	100 (Ci)	300 (Ci)	500 (Ci)	1000 (Ci)	5000 (Ci)	10000 (Ci)
2.1									
Tc-99	2.11E+05	1.30E+01	2.73E+01	2.73E+01	2.73E+01	2.73E+01	2.73E+01	2.69E+01	2.65E+01
I-129	1.57E+07	3.15E-02	6.62E-02	6.61E-02	6.61E-02	6.61E-02	6.61E-02	6.61E-02	6.61E-02
Cs-135	2.30E+06	3.45E-01	7.25E-01	7.24E-01	7.24E-01	7.24E-01	7.24E-01	7.24E-01	7.24E-01
Np-237	2.14E+06	3.15E-01	6.62E-01	8.74E-01	1.31E+00	1.63E+00	2.19E+00	2.48E+00	2.48E+00
Pu-239	2.41E+04	3.13E+02	6.57E+02	6.55E+02	6.51E+02	6.51E+02	6.41E+02	5.73E+02	4.98E+02
Pu-240	6.56E+03	5.27E+02	1.11E+03	1.11E+03	1.09E+03	1.06E+03	1.00E+03	6.57E+02	3.86E+02
Pu-242	3.73E+05	1.72E+00	3.61E+00	3.61E+00	3.61E+00	3.61E+00	3.61E+00	3.60E+00	3.55E+00
Am-241	4.33E+02	1.69E+03	3.55E+03	7.88E+03	5.75E+03	4.18E+03	1.88E+03	3.28E+00	1.38E-01
Am-243	7.38E+03	1.71E+01	3.59E+01	3.55E+01	3.49E+01	3.42E+01	3.28E+01	2.25E+01	1.40E+01



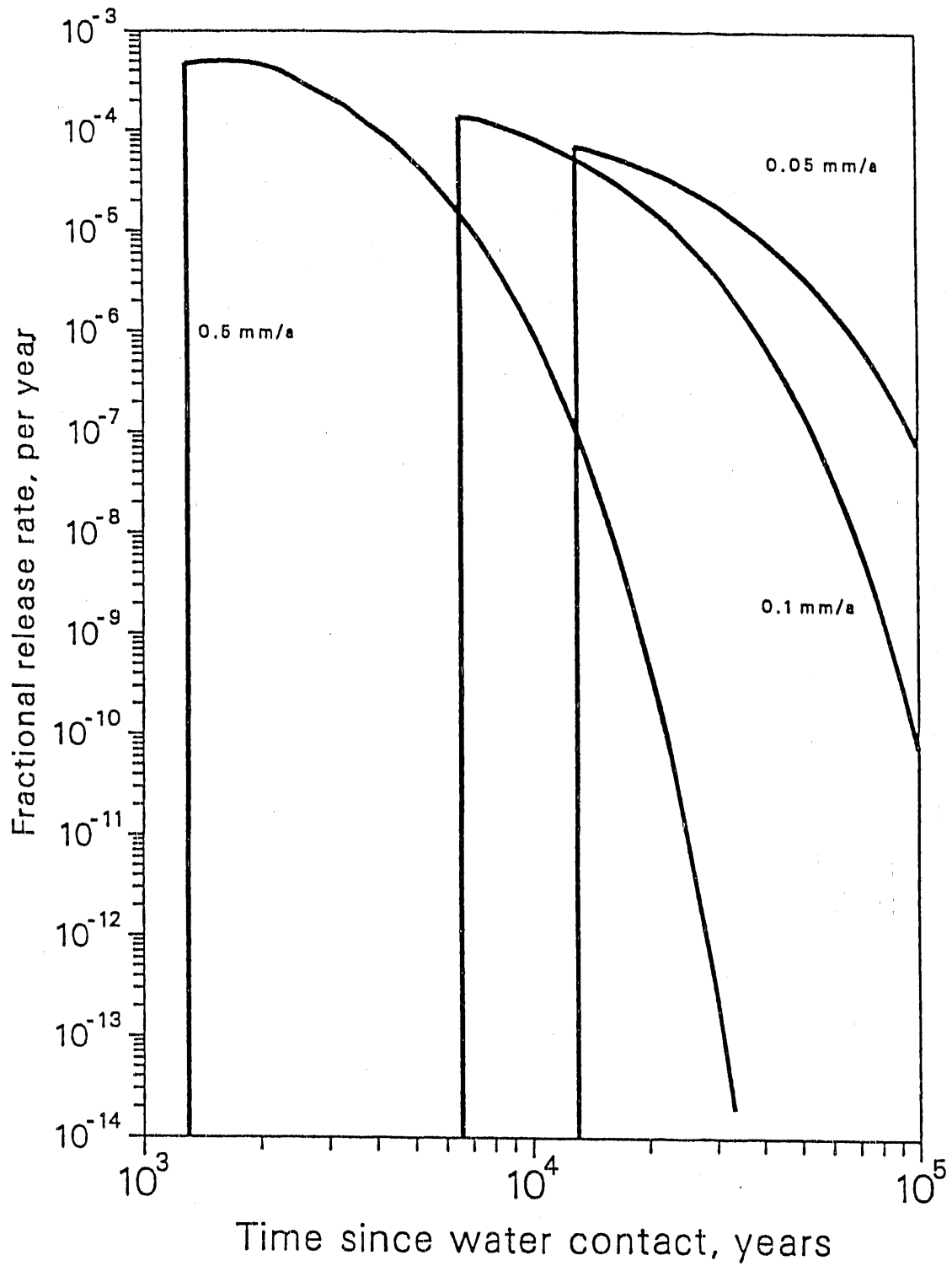


Fig. 1. Wet-drip fractional release rates of Tc-99, I-129, and Cs-135 from waste-matrix alteration, as a function of time since water contact.

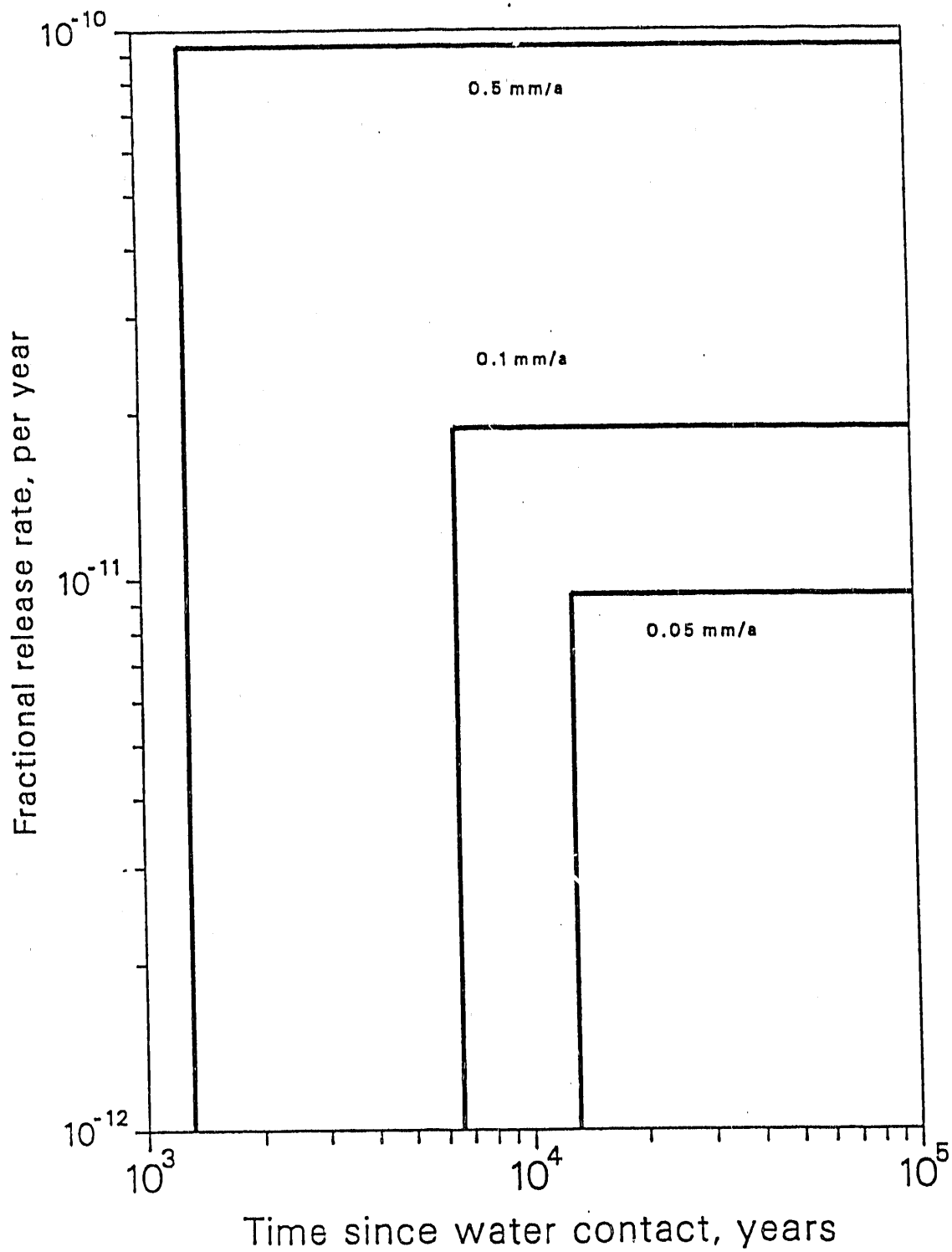


Fig. 2. Wet-drip fractional release rates of Np-237, as a function of time since water contact.

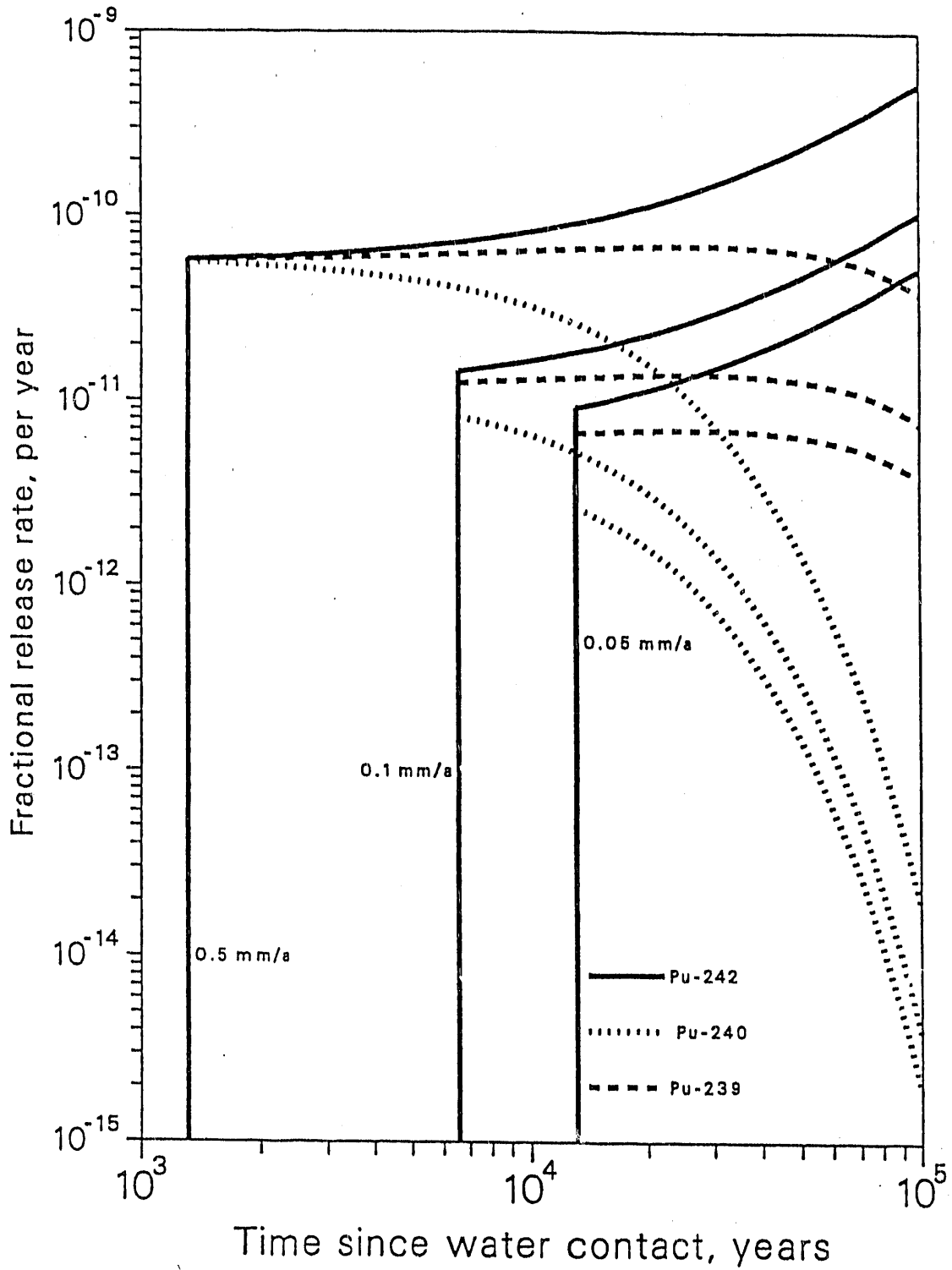


Fig. 3. Wet-drip fractional release rates of plutonium isotopes, as a function of time since water contact.

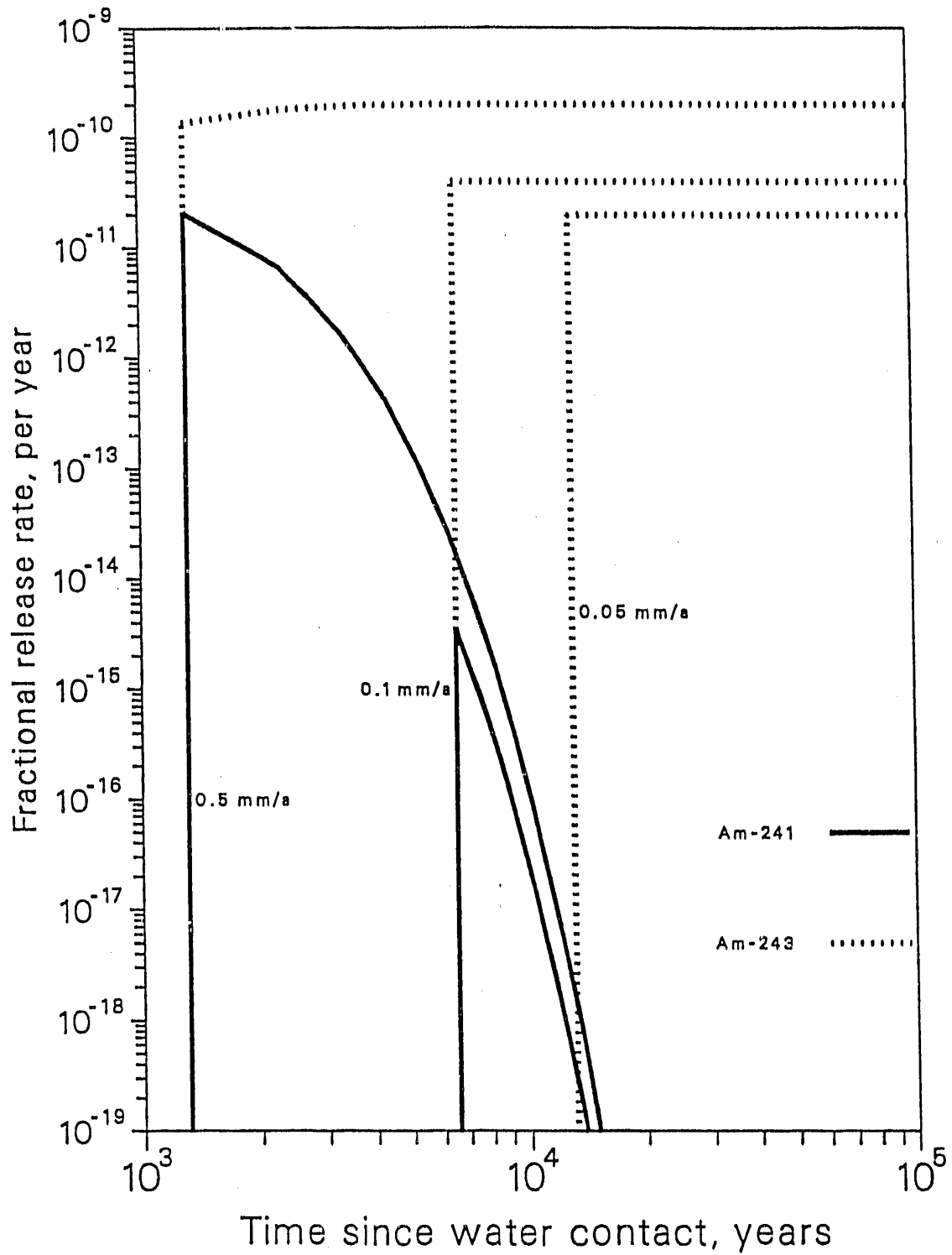


Fig. 4. Wet-drip fractional release rates of americium isotopes, as a function of time since water contact.

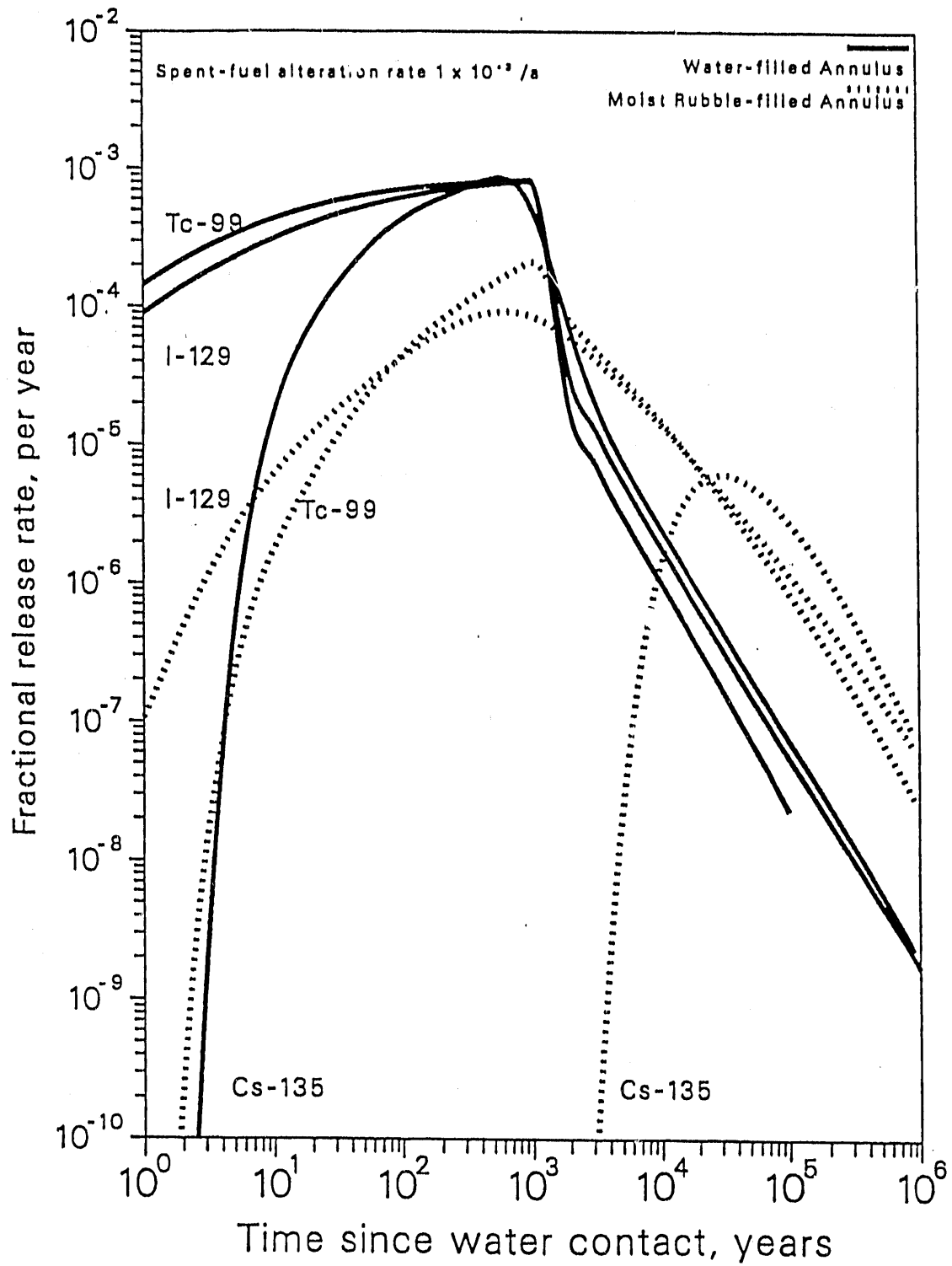


Fig. 5. Wet-continuous fractional release rates of Tc-99, I-129, and Cs-135, as a function of time since water contact.

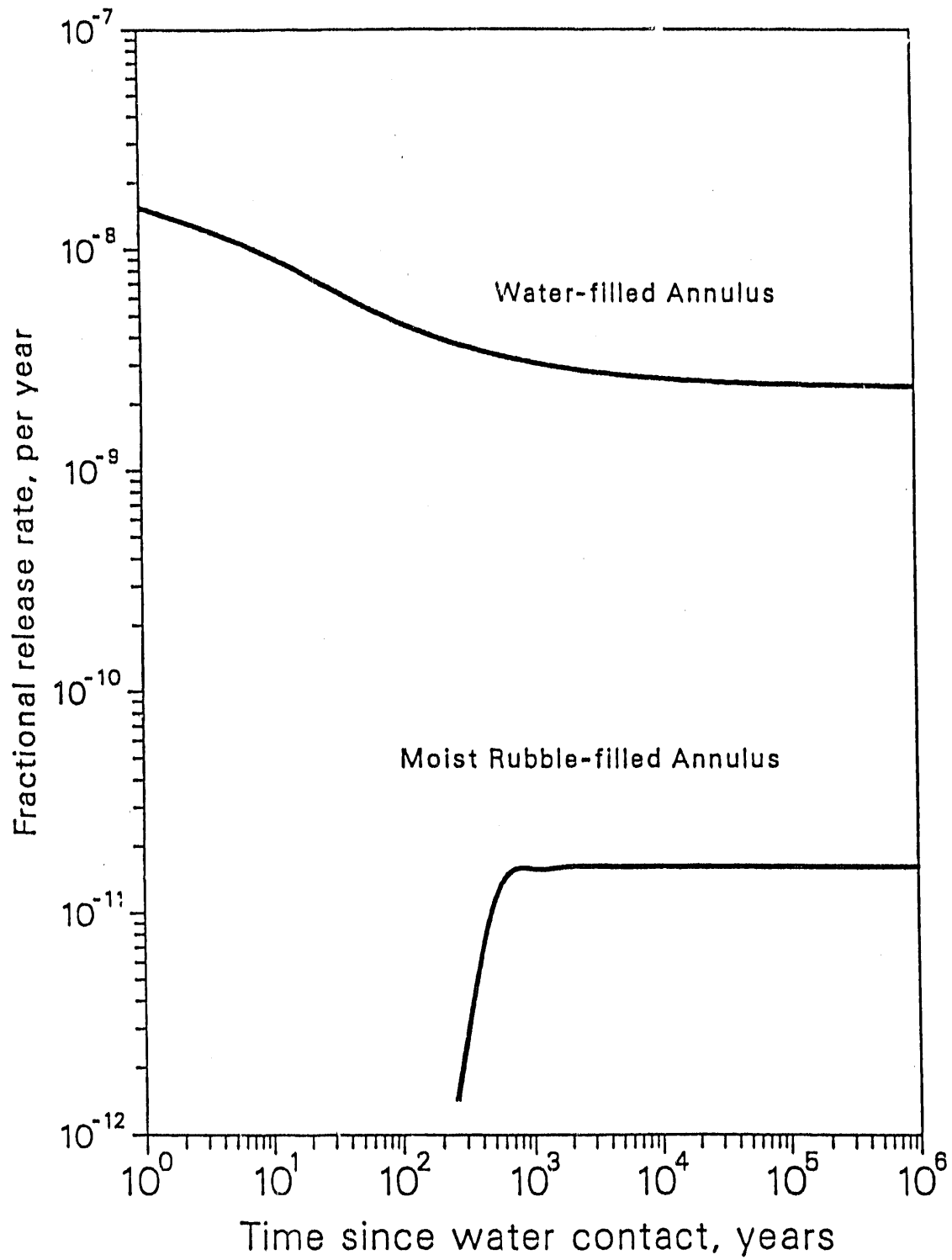


Fig. 6. Wet-continuous fractional release rates of Np-237, as a function of time since water contact.

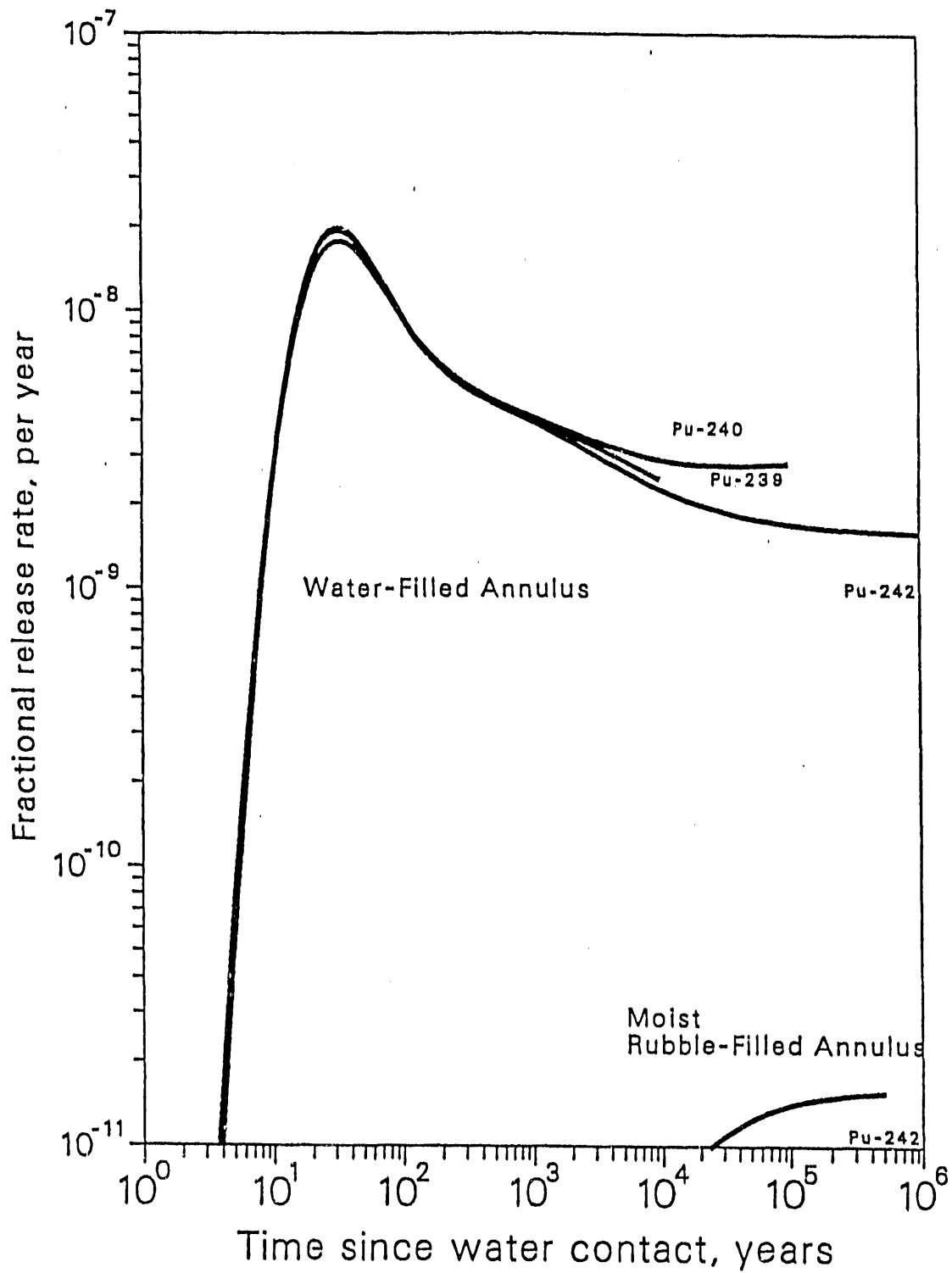
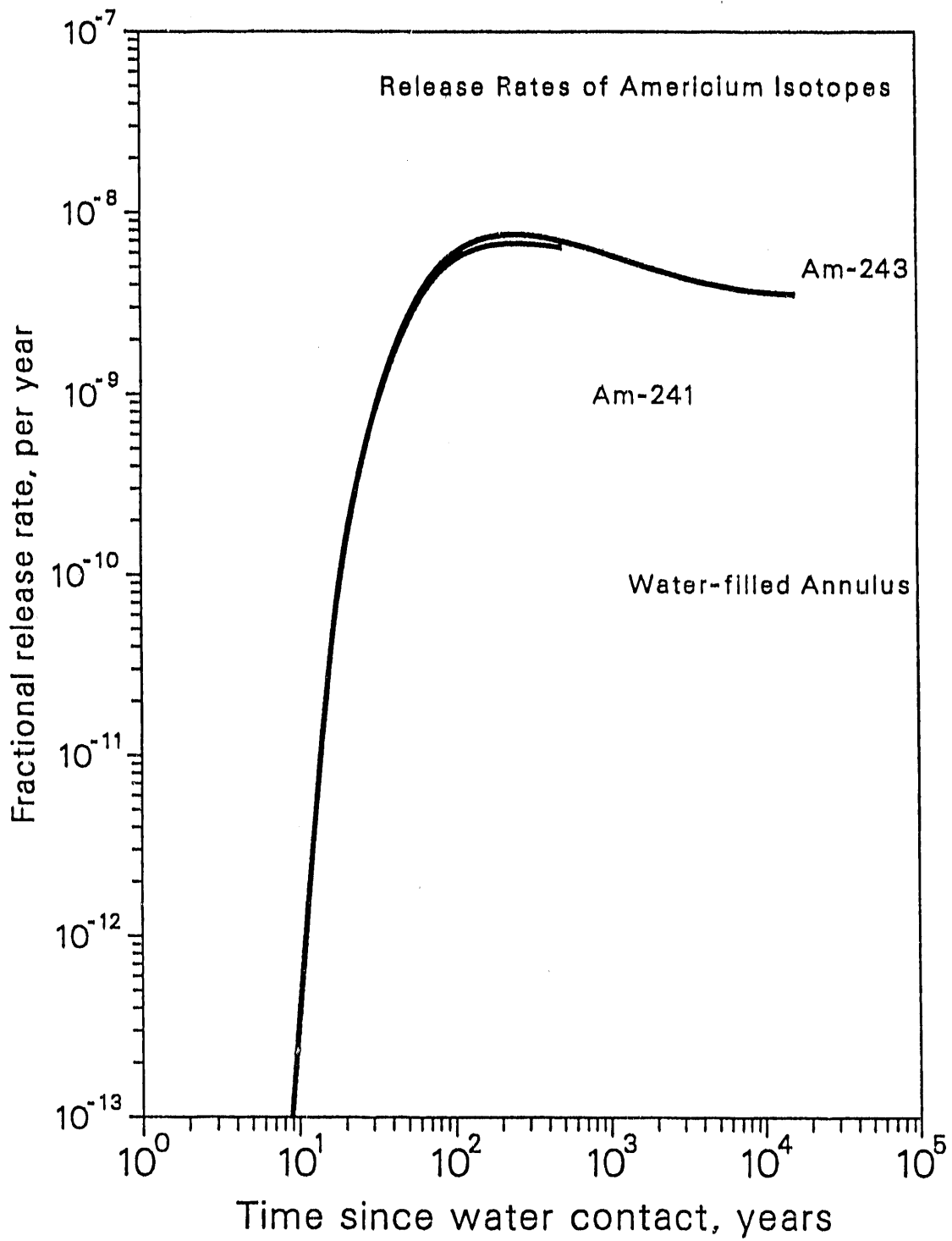


Fig. 7. Wet-continuous fractional release rates of plutonium isotopes, as a function of time since water contact.



**Fig. 8. Wet-continuous fractional release rates of americium isotopes, as a function of time since water contact.**



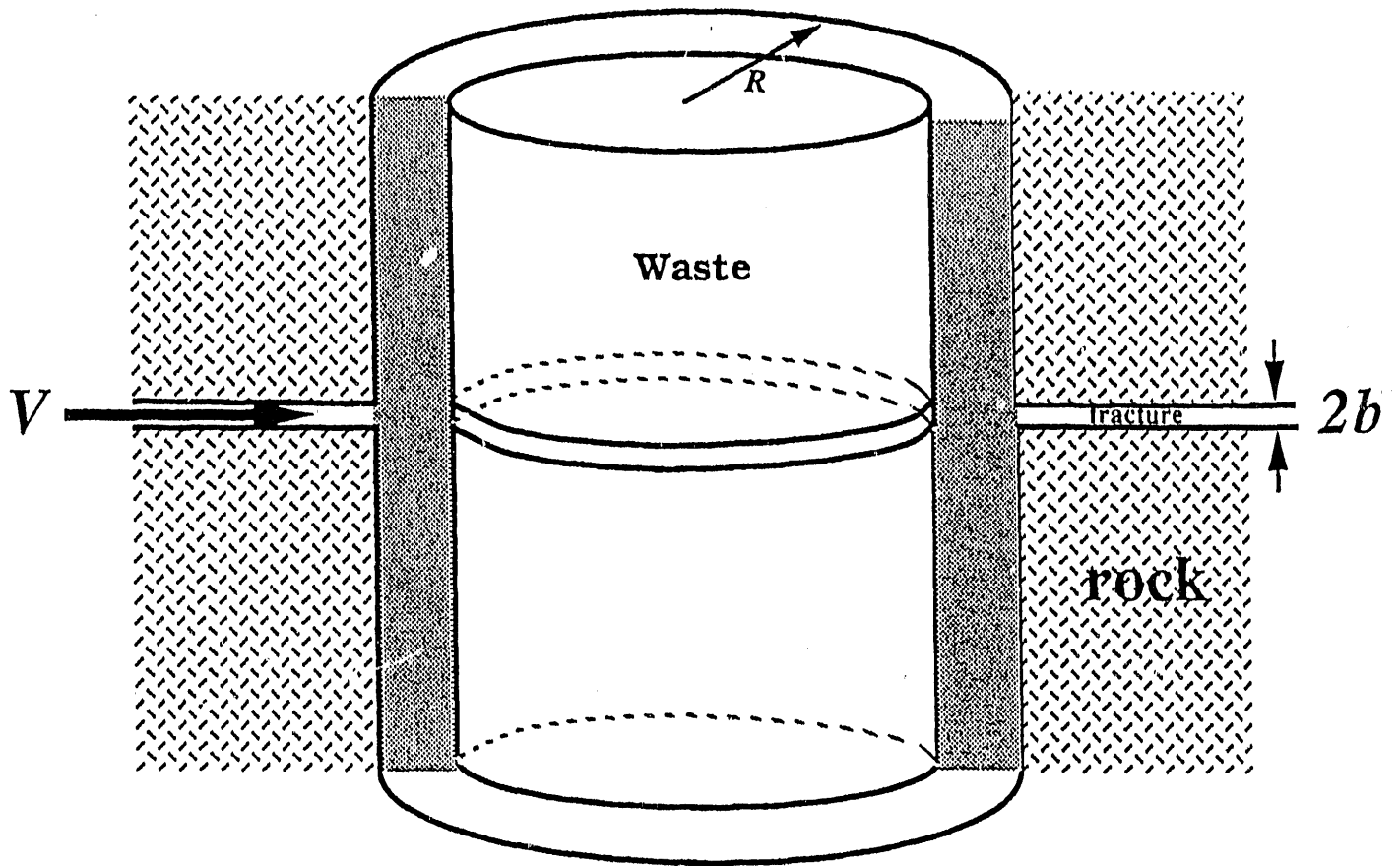


Fig. 9. A fracture intersecting a waste package.

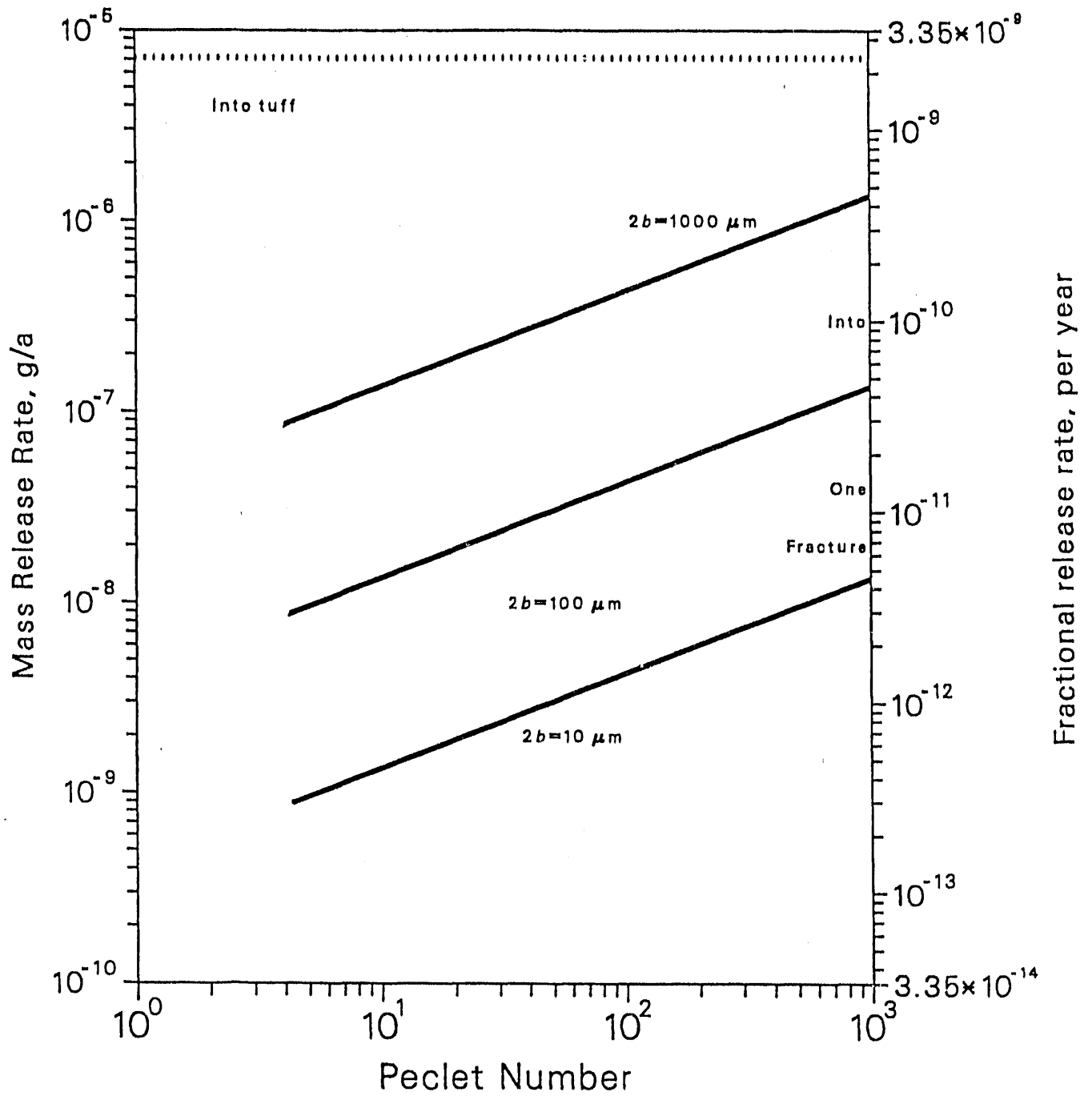


Fig. 10. Wet-continuous release rates of Np-237 into the rock matrix and into a fracture, as a function of the Peclet number for fracture flow (near steady state,  $2b =$  fracture aperture).

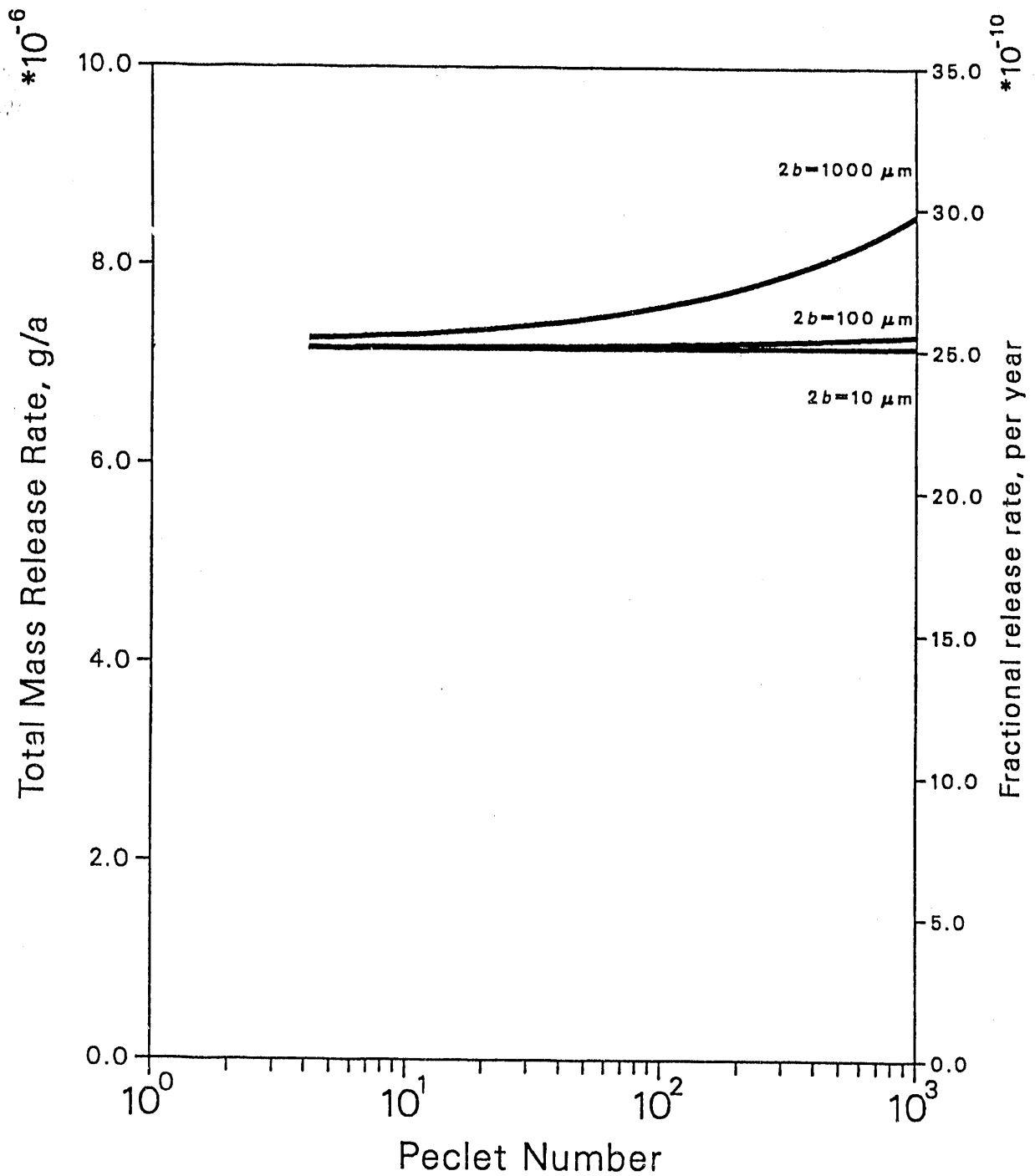


Fig. 11. Wet-continuous total release rate of Np-237 into the rock matrix and into a fracture, as a function of the Peclet number for fracture flow (near steady state,  $2b$  = fracture aperture).

**END**

**DATE  
FILMED**

**4 / 15 / 92**

